Atmospheric
Chemistry
and Physics

Using satellite observations of tropospheric NO_2 columns to infer long-term trends in US NO_x emissions: the importance of accounting for the free tropospheric NO_2 background

Rachel F. Silvern[1], **Daniel J. Jacob**[1,2], **Loretta J. Mickley**[2], **Melissa P. Sulprizio**[2], **Katherine R. Travis**[3,a],
Eloise A. Marais[4], **Ronald C. Cohen**[5,6], **Joshua L. Laughner**[5,b], **Sungyeon Choi**[7], **Joanna Joiner**[7,8], and
Lok N. Lamsal[8,9]

[1]Department of Earth and Planetary Sciences, Harvard University, Cambridge, MA, USA
[2]School of Engineering and Applied Sciences, Harvard University, Cambridge, MA, USA
[3]Department of Civil and Environmental Engineering, Massachusetts Institute of Technology, Cambridge, MA, USA
[4]Department of Physics and Astronomy, University of Leicester, Leicester, UK
[5]Department of Chemistry, University of California, Berkeley, CA, USA
[6]Department of Earth and Planetary Science, University of California, Berkeley, CA, USA
[7]Science Systems and Applications Inc., Lanham, MD, USA
[8]NASA Goddard Space Flight Center, Greenbelt, MD, USA
[9]Goddard Earth Sciences Technology and Research, Universities Space Research Association, Columbia, MD, USA
[a]now at: NASA Langley Research Center, Hampton, VA, USA
[b]now at: Division of Geological and Planetary Sciences, California Institute of Technology, Pasadena, CA, USA

Correspondence: Rachel F. Silvern (rsilvern@g.harvard.edu)

Abstract. The National Emission Inventory (NEI) of the US Environmental Protection Agency (EPA) reports a steady decrease in US NO_x emissions over the 2005–2017 period at a rate of $0.1\,Tg\,N\,a^{-1}$ (53 % decrease over the period), reflecting sustained efforts to improve air quality. Tropospheric NO_2 columns observed by the satellite-based Ozone Monitoring Instrument (OMI) over the US show a steady decrease until 2009 but a flattening afterward, which has been attributed to a flattening of NO_x emissions, contradicting the NEI. We show here that the steady 2005–2017 decrease in NO_x emissions reported by the NEI is in fact largely consistent with observed network trends of surface NO_2 and ozone concentrations. The OMI NO_2 trend is instead similar to that observed for nitrate wet deposition fluxes, which is weaker than that for anthropogenic NO_x emissions, due to a large and increasing relative contribution of non-anthropogenic background sources of NO_x (mainly lightning and soils). This is confirmed by contrasting OMI NO_2 trends in urban winter, where the background is low and OMI NO_2 shows a 2005–2017 decrease consistent with the NEI, and rural summer, where the background is high and OMI NO_2 shows no significant 2005–2017 trend. A GEOS-Chem model simulation driven by NEI emission trends for the 2005–2017 period reproduces these different trends, except for the post-2009 flattening of OMI NO_2, which we attribute to a model underestimate of free tropospheric NO_2. Better understanding is needed of the factors controlling free tropospheric NO_2 in order to relate satellite observations of tropospheric NO_2 columns to the underlying NO_x emissions and their trends. Focusing on urban winter conditions in the satellite data minimizes the effect of this free tropospheric background.

1 Introduction

Nitrogen oxide radicals ($NO_x \equiv NO + NO_2$) emitted by fuel combustion harm air quality by catalyzing ozone production and by producing nitrate particulate matter. They also contribute to acid and nitrogen deposition. Starting in the early

2000s, the US Environmental Protection Agency (EPA) implemented increasingly stringent NO$_x$ emission controls targeted principally at improving ozone air quality. The EPA National Emission Inventory (NEI) reports a steady decrease in US NO$_x$ emissions over the 2005–2017 period at a rate of 0.10 Tg N a^{-1} or 53 % overall (EPA, 2018). However, Jiang et al. (2018) showed that tropospheric NO$_2$ columns observed by the OMI satellite instrument over the US stopped decreasing after 2009, and they concluded that NO$_x$ emissions have been decreasing much less than reported by the NEI. Here we show that the flattening of the OMI NO$_2$ trend is in fact not inconsistent with the sustained decrease in NO$_x$ emissions reported by the NEI and that the NEI emission trend is consistent with other atmospheric observations of NO$_x$ and ozone trends. Our results demonstrate the importance of accounting for the free tropospheric NO$_2$ background when using satellite observations of NO$_2$ columns to infer NO$_x$ emissions and their trends.

The Ozone Monitoring Instrument (OMI) aboard the US National Aeronautics and Space Administration (NASA) Aura satellite has been making continuous daily global observations of NO$_2$ since late 2004 (Levelt et al., 2006, 2018). The NO$_2$ retrieval (Boersma et al., 2011; Bucsela et al., 2013) involves spectral fitting of measured nadir solar backscatter at 400–500 nm, yielding "slant" NO$_2$ columns along the line of sight from which the contribution from the stratosphere is removed (Martin et al., 2002; Richter and Burrows, 2002; Bucsela et al., 2013). The slant tropospheric columns are then converted to actual tropospheric NO$_2$ columns by accounting for surface and atmospheric scattering, and assuming a vertical distribution of NO$_2$ within the column ("shape factor"). In polluted regions with high NO$_x$ emissions, most of the information in the NO$_2$ tropospheric column is presumed to originate from the boundary layer. Thus, the column is commonly viewed as a proxy for NO$_x$ emissions.

Satellite observations of tropospheric NO$_2$ columns have been used extensively to infer NO$_x$ emissions and their trends (Leue et al., 2001; Martin et al., 2003; Richter et al., 2005; Boersma et al., 2008). OMI NO$_2$ observations from the early part of the record showed decreasing trends over the US consistent with the decreases in NO$_x$ emissions reported by the NEI (Russell et al., 2012; Duncan et al., 2013, 2016; Streets et al., 2013; de Foy et al., 2015; Krotkov et al., 2016) and also consistent with trends in NO$_2$ concentrations observed from surface networks (Kharol et al., 2015; Lamsal et al., 2015; Lu et al., 2015; Tong et al., 2015; Zhang et al., 2018). Several studies reported a steepening of the OMI NO$_2$ decrease during the Great Recession of 2007–2009 and a subsequent flattening attributed to economic recovery (Russell et al., 2012; Tong et al., 2015; de Foy et al., 2016). However, the analysis of the 2005–2015 record by Jiang et al. (2018) shows that the post-2009 flattening of the NO$_2$ trend extends well beyond the initial economic recovery period.

The NEI is a "bottom-up" national inventory compiled by the EPA every 3 years using continuous emission monitoring systems (CEMS) for large point sources, and estimates derived from activity data and emission factors (NO$_x$ emitted per unit of activity) for smaller and distributed sources. Emissions in 2017 estimated by EPA (2018) included 35 % from on-road mobile sources, 25 % from off-road mobile sources, 12 % from industrial point sources, and 27 % from electricity generating units (EGUs). Mobile emissions are estimated with the Motor Vehicle Emission Simulator (MOVES) model using vehicle population, vehicle miles traveled (VMT), and operating modes as inputs. Long-term trends in NO$_x$ emissions are recomputed with each new NEI release using updated emission models so that national trends are self-consistent for a given NEI version.

Many recent studies using near-source, urban, and regional observations of atmospheric NO$_x$ have found that the NEI greatly overestimates US NO$_x$ emissions (Castellanos et al., 2011; Brioude et al., 2013; Anderson et al., 2014; Goldberg et al., 2016; Souri et al., 2016; Travis et al., 2016). CEMS measurements of point sources are considered reliable but tunnel and roadside measurements show that the MOVES inventory for mobile sources may be too high (Fujita et al., 2012). Fuel-based approaches for estimating emissions from mobile sources appear to be more reliable than the MOVES VMT approach (Dallmann and Harley, 2010; McDonald et al., 2012; Kim et al., 2016). McDonald et al. (2018) showed that on-road gasoline NO$_x$ emission factors used by NEI are a factor of 2 too high compared to roadside observations and their fuel-based inventory. All these studies were conducted under summertime or warm conditions. By contrast, atmospheric observations of NO$_x$ and related species during the WINTER campaign over the northeastern US during February–March 2015 showed good agreement with the NEI (Jaeglé et al., 2018; Salmon et al., 2018).

The uncertainty regarding NEI NO$_x$ emissions suggests that the trend in these emissions could be uncertain as well. However, a flattening out of US NO$_x$ emissions over the past decade, as inferred by Jiang et al. (2018) from the OMI data, would be difficult to reconcile with observations of steady improvement in ozone air quality (Astitha et al., 2017; Chang et al., 2017), which has been attributed specifically to NO$_x$ emission controls (Hidy and Blanchard, 2015; Simon et al., 2015; Strode et al., 2015; Xing et al., 2015; Blanchard and Hidy, 2018; Li et al., 2018). Here we conduct a more comprehensive analysis of 2005–2017 trends in US NO$_x$ emissions by using the GEOS-Chem chemical transport model (Travis et al., 2016) to concurrently interpret the trends observed in OMI NO$_2$ columns, nitrogen wet deposition fluxes, and surface observations of NO$_2$ and ozone.

2 The 2005–2017 trends of OMI tropospheric NO$_2$ columns

Figure 1 shows the 2005–2017 trends of OMI tropospheric NO$_2$ columns averaged spatially and annually over the con-

tiguous US. The observations are from the NASA operational retrieval (level 2, version 3.0; Krotkov et al., 2017) after removing cloudy scenes (cloud radiance fraction > 0.5), bright surfaces (surface reflectivity > 0.3), and observations affected by the so-called row anomaly (Dobber et al., 2008). OMI is in a sun-synchronous orbit with overpass at 13:30 LT. It measures backscattered solar radiation in the nadir and off-track, with 13×24 km^2 nadir pixel resolution and global daily coverage. The retrieval fits the backscattered radiance spectrum to obtain the total slant NO$_2$ column along the line of sight from the Sun to the satellite. The stratospheric contribution to the total slant column is estimated using OMI observations over clean background and cloudy areas and applying an interpolating–filtering–smoothing algorithm (Bucsela et al., 2013). The remaining tropospheric slant column is then converted to a vertical column with an air mass factor (AMF; Palmer et al., 2001) that convolves the altitude-dependent sensitivity from atmospheric scattering (scattering weights) with the local relative vertical distribution of NO$_2$ from the Global Modeling Initiative (GMI) model (shape factor). Over continental source regions, the AMF dominates the overall retrieval error due to uncertainties in a priori NO$_2$ profiles, surface albedo, and aerosol and cloud parameters (Kleipool et al., 2008; Boersma et al., 2011; Lamsal et al., 2014; Lorente et al., 2017). We recomputed the AMFs using GEOS-Chem rather than GMI shape factors and found little difference in the mean (Fig. 1).

The OMI data show an evident flattening of NO$_2$ columns after 2009, as pointed out by Jiang et al. (2018), who also find the same flattening in alternative OMI NO$_2$ retrievals produced by KNMI (Boersma et al., 2011) and UC Berkeley (Laughner et al., 2018). NO$_2$ tropospheric columns decrease at a mean rate of 6 ± 0.5 % a^{-1} over the 2005–2009 period but then do not change significantly post-2009. We find that data for the western, central, northeastern, and southeastern US all show similar trends. Hence, we focus our analysis on the mean trends over the contiguous US, following Jiang et al. (2018).

Also shown in Fig. 1 are trends from a 13-year simulation (2005–2017) with the GEOS-Chem global chemical transport model at $0.5° \times 0.625°$ nested horizontal resolution over North America. The model is driven by NEI NO$_x$ emissions for fuel combustion, decreased by 60 % for non-EGU sources following Travis et al. (2016). It also includes NO$_x$ emissions from background (nonfuel combustion) sources, including open fires (Darmenov and da Silva, 2013), lightning (Murray et al., 2012), and soil and fertilizer (Hudman et al., 2012). Further details on the model are in the Appendix. The model NO$_2$ column averages 28 % lower than observed, due to both an underestimate in background NO$_2$, discussed below, and because the Travis et al. (2016) correction to the NEI is excessive, which we will address in a separate paper. More to the point here, the model shows a sustained decrease, averaging 3.3 ± 0.1 % a^{-1} over the 2005–2017 period, at odds with the OMI observations, though lower than

the NEI reported decrease of 5.9 % a^{-1} over the same period. Here and throughout this paper we derive linear trends by ordinary regression and express them in units of percent per annum (% a^{-1}) relative to the mean over the data period, following Jiang et al. (2018). We compute uncertainty using the bootstrapping method as the error standard deviation of the linear trend.

The weaker relative trend in the model compared to the NEI is because of the contribution from background NO$_x$ sources. Figure 1c shows the annual total US NO$_x$ emissions for 2005–2017 in the GEOS-Chem simulation. Anthropogenic emissions from fuel combustion decrease at a rate of 5.9 % a^{-1}, following the NEI trend. But these emissions account for only 61 % of total US emissions in 2005 and 42 % in 2017. Natural emissions from lightning and soils play a relatively increasing role as anthropogenic emissions decrease. They have interannual variability but no significant 2005–2017 trend. The trend of total US NO$_x$ emissions for 2005–2017 in GEOS-Chem is -3.5 % a^{-1}, closely matching the simulated NO$_2$ column trend.

Trends in the NO$_x$ chemical lifetime over the 2005–2017 period would affect the relationship between trends in NO$_x$ emissions and atmospheric NO$_2$. Many factors could contribute to a trend in NO$_x$ lifetime (Laughner, 2018; Laughner and Cohen, 2018). We find in GEOS-Chem that the daily tropospheric NO$_2$ column lifetime over the contiguous US is 8.1 h in 2005 (annual mean) and 7.7 h in 2017. In the model at least, the trend in NO$_x$ lifetime is much weaker than the trend in emissions, so that the trend in concentrations mainly follows that of emissions.

3 The 2005–2017 trends of surface observations

Long-term records of surface NO$_2$ concentrations over the US are available at a large number of monitoring sites from the US EPA Air Quality System (AQS) (https://www.epa.gov/aqs, last access: 4 September 2018; Demerjian, 2000) and at additional sites in the southeast from the Southeastern Aerosol Research and Characterization Study (SEARCH) network (https://www.dropbox.com/sh/o9hxoa4wlo97zpe/AACbm6LetQowrpUgX4vUxnoDa?dl=0, last access: 27 July 2018; Hansen et al., 2003; Edgerton et al., 2006). AQS sites are mainly urban and measure NO$_2$ with a chemiluminescence analyzer equipped with a molybdenum converter, known to have positive interferences from NO$_x$ oxidation products including peroxyacetyl nitrate (PAN) and nitric acid (HNO$_3$; Dunlea et al., 2007; Steinbacher et al., 2007; Reed et al., 2016). SEARCH sites are both urban and rural and use a more specific photolytic converter instrument in which broadband photolysis of NO$_2$ is followed by chemiluminescence detection of the NO product with accuracy better than 10 % (Ryerson et al., 2000; Pollack et al., 2010).
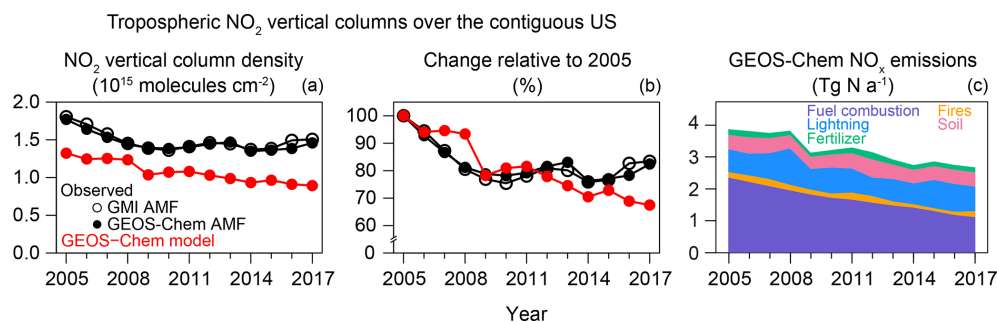
Tropospheric NO$_2$ vertical columns over the contiguous US

Figure 1. The 2005–2017 trends in tropospheric NO$_2$ columns and NO$_x$ emissions over the contiguous US. Panel **(a)** shows OMI observations averaged over the contiguous US and the corresponding GEOS-Chem simulation. The OMI observations are from the NASA retrieval (Krotkov et al., 2017) with air mass factors (AMFs) computed from the original GMI model NO$_2$ vertical profiles or GEOS-Chem vertical profiles. Panel **(b)** shows percent changes in tropospheric NO$_2$ columns relative to 2005. Panel **(c)** shows 2005–2017 annual total NO$_x$ emissions from the GEOS-Chem model, including anthropogenic fuel combustion emissions from the National Emission Inventory (NEI), with a 60 % decrease for non-EGU sources (see text and Appendix).

Figure 2a–d show annual average trends in daily surface NO$_2$ concentrations at the 132 AQS sites with continuous yearlong records for 2005–2017 and the 2 rural SEARCH sites (Centreville, AL, and Yorkville, GA) with continuous records for 2005–2016 (SEARCH was discontinued in 2017). Also shown for the AQS sites are the values corrected for interferences based on local GEOS-Chem monthly mean NO$_2$, alkyl nitrate, PAN, and HNO$_3$ concentrations and following the correction factor in Lamsal et al. (2008). The AQS data show decreasing trends throughout the 2005–2017 period, generally consistent with the NEI. The rural SEARCH sites also show a steady decrease but are more noisy (only two sites). One would expect the trend in the urban AQS data to be most indicative of the trend in anthropogenic NO$_x$ emissions from fuel combustion. GEOS-Chem underestimates the AQS observations because of the urban nature of the sites, but the model relative decreases agree closely with observations for both the AQS and the SEARCH data. This is in sharp contrast to the OMI NO$_2$ data.

Jiang et al. (2018) reported AQS surface NO$_2$ trends of -6.6 ± 1.4 % a^{-1} for 2005–2009 and -2.6 ± 1.5 % a^{-1} for 2011–2015, indicating a significant weakening of the trend with time. But they used all AQS sites in that analysis including those with incomplete records. We find that when using only sites with continuous records, the slope is steeper for the latter time period. Specifically, we find the AQS trend to be -6.6 ± 1.2 % a^{-1} for 2005–2009 and -4.5 ± 1.7 % a^{-1} for 2011–2015. In comparison, the NEI emission trend is -6.4 % a^{-1} for 2005–2009 and -5.3 % a^{-1} for 2011–2015. Thus, the surface data suggest a slight weakening of the NO$_x$ emission trend relative to the NEI but not the flattening implied by the OMI data. Jiang et al. (2018) presented an alternative fuel-based NO$_x$ emission inventory to the NEI, featuring a slowdown in the trend of US NO$_x$ emissions after 2009 due to a slower rate of reduction for industrial, off-road mobile, and on-road diesel sources as well as a smaller relative contribution of on-road gasoline. That inventory shows a

-2.9 % a^{-1} trend for 2011–2015. The AQS trend is in somewhat better agreement with the NEI inventory but could accommodate either inventory within its error standard deviation.

Figure 2e–f show observed and simulated trends in nitrate (NO$_3^-$) wet deposition fluxes for the 138 National Acid Deposition Program (NADP; https://nadp.slh.wisc.edu/data/NTN/, last access: 14 August 2018) sites with continuous yearlong records for 2005–2017. Nitric acid gas and nitrate aerosol are both efficiently scavenged by precipitation and the lifetime of NO$_x$ is sufficiently short that nitrate wet deposition fluxes should relate to total NO$_x$ emissions. The relationship is not one-to-one because of competition from dry deposition but one would not expect a long-term trend in the wet/dry deposition ratio. GEOS-Chem model values for individual years are corrected for precipitation bias using the high-resolution PRISM precipitation data (http://prism.oregonstate.edu, last access: 14 August 2018; Di Luzio et al., 2008), as described by Paulot et al. (2014) and Travis et al. (2016). Model values average 17 % lower than observed values, again because the model may underestimate emissions, but the trends are consistent. The fluxes show a decrease over the 2005–2017 time period (averaging 2.7 ± 0.3 % a^{-1} observed, 2.9 ± 0.3 % a^{-1} modeled), weaker than for surface NO$_2$ concentrations. After 2012, there is still a significant decrease in nitrate wet deposition, though it is less than during the earlier time period (averaging 1.3 ± 0.9 % a^{-1} observed and 1.7 ± 0.7 % a^{-1} modeled).

Nitrate wet deposition is more sensitive to background (nonfuel combustion) influences than NO$_2$ concentrations because (1) the wet deposition sites are prevailingly rural and (2) precipitation scavenges a deeper column. Indeed, in GEOS-Chem, the mean nitrate wet deposition trend is more consistent with the -3.5 % a^{-1} trend of total NO$_x$ emissions (including lightning and soils) than that of emissions from fuel combustion (-5.9% a^{-1}).
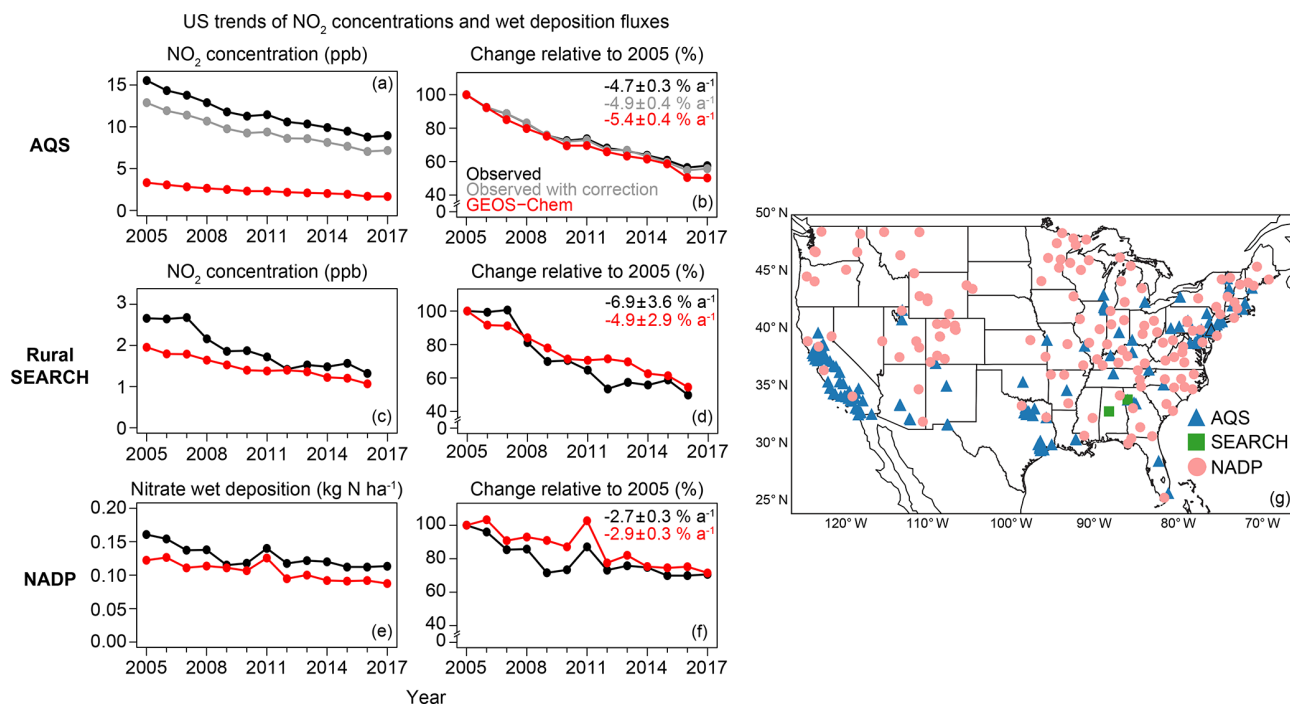
Figure 2. The 2005–2017 trends in annual mean surface NO$_2$ concentrations and nitrate wet deposition fluxes over the contiguous US. Observations are compared to GEOS-Chem model values sampled at the corresponding sites. The map in the right panel **(g)** shows the observation sites for the AQS, SEARCH, and NADP measurements networks with continuous annual records for 2005–2017 (2016 for SEARCH). Panels **(a)** and **(b)** show surface NO$_2$ observed at AQS sites (mainly urban). The measurements are affected by positive interference from NO$_x$ oxidation products and the gray line shows the data corrected as in Lamsal et al. (2008). Panels **(c)** and **(d)** show surface NO$_2$ at the two rural SEARCH sites in the southeastern US. Panels **(e)** and **(f)** shows nitrate wet deposition fluxes at NADP sites. Panels **(b)**, **(d)** and **(f)** show trends relative to 2005 values and the mean ± standard deviation percent change per year is shown inset. All trends shown are statistically significant.

The relative contribution from background sources to nitrate wet deposition would be expected to increase over time as fuel combustion emissions decrease. In order to quantify this, we performed GEOS-Chem sensitivity simulations for 2005 and 2017 with only background NO$_x$ emissions (shutting off NO$_x$ emissions from US fuel combustion). We find that background contributed 50 % of nitrate wet deposition at NADP sites in 2005 but 69 % in 2017. In contrast, background only contributed 5 % to surface NO$_2$ at AQS sites in 2005 and 10 % in 2017.

Figure 3 shows summertime ozone trends for 2005–2017 as further evidence of a sustained decrease in anthropogenic NO$_x$ emissions. Data are from the AQS and Clean Air Status and Trends Network (CASTNET; https://www.epa. gov/castnet, last access: 27 July 2018) networks. We show records for the 47 CASTNET and 427 AQS sites with continuous summertime records for 2005–2017. The trends are for the 95th percentiles in the maximum daily 8 h average (MDA8) values determined at individual sites and then averaged across all sites for each summer. We excluded high-elevation (> 1.5 km) CASTNET sites in the western US because they have different trends driven in part by the larger influence from background ozone (Cooper et al., 2011; Lin

et al., 2017; Jaffe et al., 2018). Much of the interannual variability in ozone concentrations in Fig. 3 can be explained by surface temperatures, including the 2012 peak in ozone in the observations and captured by GEOS-Chem, which is due to anomalously high temperatures (Fiore et al., 2015; Jia et al., 2016; Lin et al., 2017). Nonetheless, the surface observations do show overall decreases over the 2005–2017 time period. On a national scale, the observations show declines of 1.11 ± 0.08 ppb a^{-1} (CASTNET) and 1.04 ± 0.03 ppb a^{-1} (AQS), with no indication of a post-2009 flattening. The GEOS-Chem model shows similar trends. The sustained (post-2009) decrease in ozone pollution over the past decade provides additional evidence of a continued decrease in anthropogenic NO$_x$ emissions.

4   Comparative analysis of trends

Figure 4 combines the relative trends since 2005 of NEI NO$_x$ emissions, OMI tropospheric NO$_2$ columns, surface NO$_2$ concentrations, and nitrate wet deposition fluxes into a single plot. Observed surface NO$_2$ concentrations follow the NEI emissions trend, showing consistency with a sustained
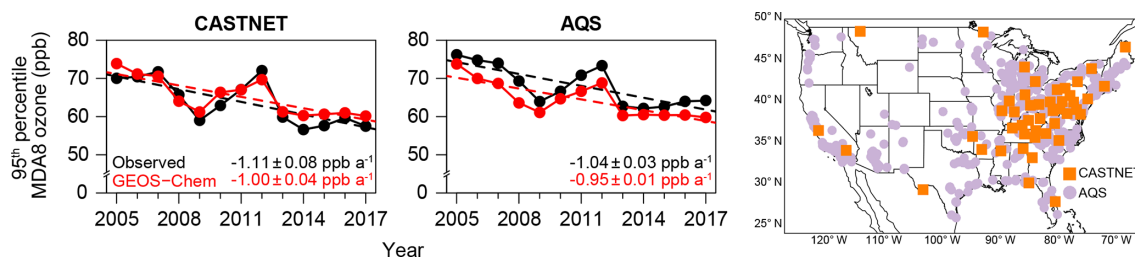
Figure 3. Summertime surface ozone trends for 2005–2017 at the CASTNET and AQS networks in the contiguous US. The trends are for the 95th percentile of the maximum daily 8 h average (MDA8) ozone concentrations computed for individual sites (shown in the map on the right) and then averaged over all sites from the network. High-elevation (> 1.5 km) CASTNET sites in the western US are excluded. The slope and standard deviation of the linear regressions are shown inset, and all trends shown are statistically significant.

Figure 4. Relative trends since 2005 of NEI NO$_x$ emissions and relevant atmospheric quantities averaged over the contiguous US. Panel **(a)** shows observations and **(b)** shows the GEOS-Chem simulation. NEI NO$_x$ emissions are the same in both panels. The SEARCH network was discontinued in 2017.

decline of emissions over the 2005–2017 time period. This behavior is well captured by GEOS-Chem, which confirms the 1 : 1 relationship expected between surface NO$_2$ concentrations and NO$_x$ emissions. Nitrate wet deposition observations show a much weaker trend, which we attributed in Sect. 3 to a larger contribution of the background. The GEOS-Chem trend for nitrate wet deposition and tropospheric NO$_2$ columns is similarly weaker than for surface NO$_2$, reflecting the influence of the background, but shows a steeper decrease than observed after 2009. This suggests that GEOS-Chem may underestimate the background contribution.

Satellite-based tropospheric NO$_2$ columns show trends remarkably similar to those of nitrate wet deposition fluxes, both in the OMI observations and in GEOS-Chem, suggesting that the post-2009 flattening of the OMI trend is due to a large and increasing relative influence of the background rather than to a leveling of US NO$_x$ emissions.

5 Background contribution to OMI NO$_2$ trends

We showed in Sect. 4 that the 2005–2017 trend of OMI NO$_2$ columns over the US is similar to that of nitrate wet deposition and much weaker than that of surface NO$_2$ concentrations, pointing to the importance of background in affecting the NO$_2$ column. To further examine this effect, we segregated the OMI observations into winter and summer as well as urban and rural. Urban conditions are defined as the top 10 % NO$_x$-emitting $0.5° \times 0.625°$ grid squares in the US according to the NEI. We expect background influences to be relatively higher at rural than urban sites, and higher in summer (lightning, soil, intercontinental transport; Fischer et al., 2014) than in winter. Thus, background influences should be at a minimum in winter urban conditions and a maximum under summer rural conditions.

Figure 5 shows the results. OMI NO$_2$ observations in urban winter show a steady decline at a mean rate of $3.3 \pm 0.5 \% \, a^{-1}$, with no post-2009 flattening, though there is some suggestion of a slightly weaker trend after 2009 when compared to GEOS-Chem driven by NEI. By contrast, the OMI NO$_2$ observations in rural summer show no significant trend over the 2005–2017 period. GEOS-Chem for rural summer shows a significant decreasing trend for 2005–2017 but weaker than for urban winter and become insignificant for the 2009–2017 period. The winter rural and summer urban conditions in Fig. 5 show trends that are intermediate between these two limiting cases. The ability of GEOS-Chem to capture the observed post-2009 weakening of the trend in the summer urban case argues against a seasonal flattening of emissions that would affect summer but not winter.

It thus appears that the post-2009 flattening of the OMI NO$_2$ trend over the US is due to increasing relative importance of the NO$_2$ background, rather than to flattening of US NO$_x$ emissions. Satellite observations of tropospheric NO$_2$ columns are more sensitive to the free troposphere than to the boundary layer because of atmospheric scattering; the sensitivity increases by a factor of 3 from the surface to the upper troposphere for clear sky and by much more for a cloudy atmosphere (Martin et al., 2002). For the OMI NO$_2$ data set
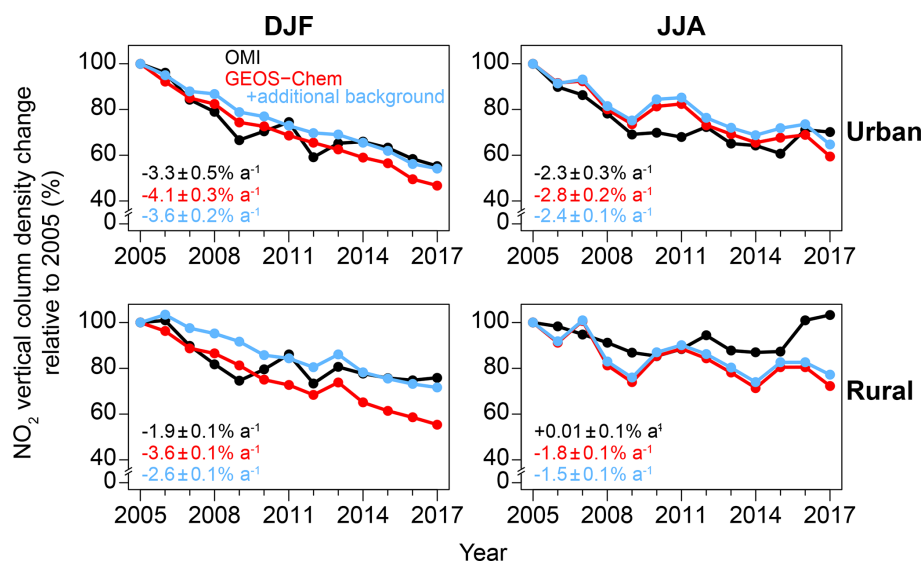
Figure 5. OMI tropospheric NO$_2$ column trends over the contiguous US relative to 2005, separated into urban and rural as well as summer (JJA) and winter (DJF). OMI observations are shown in black, the standard GEOS-Chem model simulation with EPA National Emission Inventory (NEI) trends (EPA, 2018) is in red, and the GEOS-Chem sensitivity simulation with additional NO$_2$ background (50 ppt above 5 km in winter and above 10 km in summer, up to the local tropopause) is shown in blue. Slopes and standard deviation of the linear regressions are shown inset. Urban conditions are defined as the top 10 % NO$_x$-emitting 0.5° × 0.625° grid squares in the NEI.

used here, the sensitivity increases by over a factor of 4 from the surface to the upper troposphere on average, as given by the scattering weights (Krotkov et al., 2017). The AMF is intended to correct for this effect but relies on an assumed model vertical distribution of NO$_2$ that may not correctly account for free tropospheric levels or for the changing ratio between the free troposphere and the boundary layer as anthropogenic NO$_x$ emissions decrease.

There is indeed evidence that free tropospheric NO$_2$ makes a large contribution to OMI NO$_2$ columns and that models underestimate this contribution. Measurements of NO$_2$ vertical profiles during the SEAC^{4}RS aircraft campaign over the southeastern US in August–September 2013 showed a median concentration of 300 ppt near the surface, dropping to a 50 ppt background in the free troposphere at 2–10 km, and rising back to 130 ppt at the 12 km aircraft ceiling (Silvern et al., 2018). By applying OMI scattering weights to this median vertical profile, most representative of a rural profile, Travis et al. (2016) found that the boundary layer below 1.5 km contributed only 19 %–28 % of the OMI NO$_2$ tropospheric column. A GEOS-Chem simulation of the SEAC^{4}RS conditions matched the observed 50 ppt background (mostly from lightning) but could not reproduce the enhancement above 10 km (Travis et al., 2016; Silvern et al., 2018). The GMI model used to compute AMFs in the NASA OMI NO$_2$ retrievals also has little NO$_2$ in the upper troposphere (Lamsal et al., 2014). Measurements of NO$_2$ in the upper troposphere are prone to positive interferences because of inlet decomposition of labile reservoirs (Reed et al., 2016), but the measurements in SEAC^{4}RS were designed to minimize

and correct for these interferences (Thornton et al., 2000; Day et al., 2002; Wooldridge et al., 2010; Nault et al., 2015). Silvern et al. (2018) suggested that errors in the kinetics of NO–NO$_2$–O$_3$ cycling reactions could explain model underestimates of NO$_2$ concentrations in the upper troposphere.

Choi et al. (2014) and Belmonte Rivas et al. (2015) used the so-called cloud-slicing method to isolate the upper tropospheric contribution to the OMI NO$_2$ observations by comparing neighboring cloudy scenes with cloud tops at different altitudes. They report in this manner partial NO$_2$ columns at 6–10 km altitude. Marais et al. (2018) evaluated these data in comparison with aircraft observations and found large uncertainties but concluded that GEOS-Chem underestimates NO$_2$ at 6–10 km over North America by 20–30 ppt in winter with no significant bias in summer. The good agreement in summer is consistent with the comparison to SEAC^{4}RS observations, which shows, however, a low model bias above 10 km.

We conducted a sensitivity test, adding 50 ppt of background NO$_2$ to the GEOS-Chem vertical profiles above 5 km altitude in winter and above 10 km in summer, up to the local tropopause. The resulting normalized vertical profiles (shape factors) were convolved with the vertical distribution of sensitivities (scattering weights) provided by the NASA retrieval to recompute the AMFs. The implications for the model trends are shown in Fig. 5 as the blue lines. The effect is large for winter rural conditions, where the added free tropospheric background is particularly important and largely reconciles the model trend with the OMI observations. It is much less in summer, where the addition is only above 10 km

and there is already substantial background NO$_2$ present. The discrepancy between the model and the observations in summer is largely driven by the uptick in the summer rural observations for 2016–2017.

It is possible that additional background NO$_2$ missing from the model in summer could be present in the tropopause region and lower stratosphere. The deepest convection in summertime over the US can reach 17 km in the lowermost stratosphere (Randel et al., 2012; Huntrieser et al., 2016b; Anderson et al., 2017; Herman et al., 2017; Smith et al., 2017). Such a deep convective injection could conceivably deliver substantial lightning NO$_2$ above the tropopause. Although delivered above the tropopause, this NO$_2$ would be counted as tropospheric in retrievals because it would represent an enhancement above background NO$_2$ columns in the stratospheric separation. It could have a particularly important effect on the AMF by being delivered above clouds. High NO$_x$ mixing ratios in the lowermost stratosphere were observed over the central and southeastern US during the DC3 aircraft campaign in May–June 2012 and were attributed to lightning (Huntrieser et al., 2016a, b), and higher lightning flash rates have been observed in tropopause-penetrating above-anvil cirrus plumes (Bedka et al., 2018). There is suggestive evidence that convective injection into the lowermost stratosphere over the US may have increased during the 2004–2013 period (Cooney et al., 2018), which could further affect the OMI NO$_2$ column trend, although the Lightning Imaging Sensor (LIS) satellite data do not show a 2003–2012 trend in total lightning over the US (Koshak et al., 2015). While tropopause heights in the GEOS MERRA-2 meteorological data driving GEOS-Chem agree well with SEAC^{4}RS observations of water vapor and ozone (Kuang et al., 2017; Smith et al., 2017), models in general do not properly capture the observed convective injections into the lowermost stratosphere (Smith et al., 2017; Anderson et al., 2019). The 0.5° × 0.625° resolution of the MERRA-2 meteorological data would be too coarse to resolve convective overshoots.

6 Conclusions

US emissions of nitrogen oxides (NO$_x$ ≡ NO + NO$_2$) from fuel combustion steadily declined over 2005–2017 at a mean rate of 5.9 % a^{-1} according to the National Emission Inventory (NEI) of the US EPA. Tropospheric NO$_2$ columns over the US observed by OMI aboard the Aura satellite instead show a leveling off after 2009, leading to the suggestion that the NEI emission trend is in error and that related air quality gains have halted. Here we re-examined this issue by using trends in surface observations together with a 2005–2017 GEOS-Chem chemical transport model simulation to better understand the relationship between satellite NO$_2$ observations, NO$_x$ emissions, and their trends.

We started by comparing the 2005–2017 GEOS-Chem simulation driven by NEI emission trends to the OMI observations. The model shows a sustained decrease in the tropospheric NO$_2$ column at a mean rate of 3.3±0.1 % a^{-1} over the period. The rate is less than the NEI trend because of natural NO$_x$ emissions (mainly from lightning and soils) that account in GEOS-Chem for 58 % of total NO$_x$ emissions over the US by 2017. Nevertheless, the GEOS-Chem simulation cannot capture the post-2009 flattening in the OMI observations.

We then examined 2005–2017 US trends in surface observations of NO$_2$ concentrations and nitrate wet deposition fluxes from surface networks (AQS, SEARCH, NADP). Surface NO$_2$ concentrations measured by the AQS (urban) and SEARCH (rural) surface networks show a decline over the 2005–2017 time period that closely follows the NEI emissions trend, and the same is found in GEOS-Chem. Some deviation between AQS NO$_2$ and the NEI towards the later part of the time period suggests that the rate of decrease in emissions may have slowed slightly. Nitrate wet deposition shows a much weaker 2005–2017 trend than surface NO$_2$ and NEI emissions, both in the observations and the model, reflecting a large and increasing relative contribution from background sources (69 % in the model in 2017) as anthropogenic emissions decrease. Surface ozone concentrations from the CASTNET and AQS networks show sustained 2005–2017 decreases, consistent with the model; such sustained decreases would be hard to reconcile with a flattening of NO$_x$ emissions.

Bringing together these observed trends, we see two different patterns: (1) a 2005–2017 decrease in surface NO$_2$ that supports the steady decrease in NO$_x$ emissions reported by the EPA NEI and (2) a weaker trend and post-2009 flattening of OMI NO$_2$ and nitrate wet deposition that reflects a growing influence from the background, rather than large error in NEI NO$_x$ emissions.

We confirmed the importance of background NO$_2$ in driving the post-2009 flattening of OMI NO$_2$ trends over the US by segregating the OMI observations into urban and rural as well as winter and summer. There is a steady 2005–2017 decrease in the urban winter data where background influence is lowest. By contrast, there is no significant 2005–2017 trend in rural summer (where background influence is highest). The failure of GEOS-Chem to reproduce the observed post-2009 flattening then points to a model underestimate of the NO$_2$ background. Cloud-sliced OMI NO$_2$ data indicate a GEOS-Chem underestimate of the upper tropospheric background in winter. Deep convective injections of lightning NO$_x$ above the tropopause might add to the NO$_2$ background in summer. Observations from the NASA SEAC^{4}RS aircraft campaign show lower NO / NO$_2$ ratios than simulated by GEOS-Chem, which could reflect errors in the kinetics of NO–NO$_2$–O$_3$ chemical cycling (Silvern et al., 2018). While such errors would be most important in summertime, chemistry important for wintertime NO$_x$ not being comprehensively included in models may help to explain the winter background NO$_2$ underestimate. Observa-

tions of short-chained alkyl nitrates show higher concentrations in the northern extratropical free troposphere in winter than captured by GEOS-Chem and may represent an increasing reservoir of background NO$_x$ (Fisher et al., 2018). Measurements from the WINTER campaign suggest models may also overestimate NO$_x$ loss via N$_2$O$_5$ hydrolysis (Jaeglé et al., 2018; Kenagy et al., 2018; McDuffie et al., 2018), and recent laboratory data suggest that models using the recommended NASA-JPL kinetics for the NO$_2$ + OH reaction may overestimate NO$_x$ loss at cold temperatures (Amedro et al., 2019).

We conclude that the sustained 2005–2017 decrease in US NO$_x$ emissions reported by the EPA is supported by observations and that better understanding of the free tropospheric background is needed to interpret satellite observations of NO$_2$ tropospheric columns in terms of their implications for NO$_x$ emissions and their trends. The concern is minor in highly polluted areas where NO$_x$ emissions are sufficiently high to dominate over the background influence. In the US, however, NO$_x$ emissions have now decreased to the point that NO$_2$ columns over nonurban areas are mostly contributed by the free tropospheric background. Accounting for this poorly understood background will become increasingly important as NO$_x$ emissions continue to decrease in the developed world and in tropical regions that are undergoing rapid development but have a deep troposphere and intense lightning.

Appendix A: The GEOS-Chem model

We conducted a 13-year simulation (2005–2017) with the GEOS-Chem global 3-D chemical transport model version 11-02c (http://www.geos-chem.org, last access: 14 August 2018) using NASA MERRA-2 assimilated meteorological data (Gelaro et al., 2017). We use the nested North American version of GEOS-Chem at the native MERRA-2 $0.5° \times 0.625°$ horizontal resolution over North America and adjacent oceans (10–70° N, 140–40° W) with dynamic boundary conditions from a global simulation with $4° \times 5°$ horizontal resolution. The simulation includes detailed NO$_x$–hydrocarbon–aerosol chemistry as described in Travis et al. (2016), Fisher et al. (2016) and Marais et al. (2016). US anthropogenic emissions are distributed spatially following the NEI2011 inventory (EPA, 2018). NEI2011 is scaled for individual years using national annual totals (EPA, 2018), and we decrease non-EGU NO$_x$ emissions by 60 %, as in Travis et al. (2016), for all years. Open fire emissions are from the daily Quick Fire Emissions Database (QFED; Darmenov and da Silva, 2013) with diurnal variability from the Western Regional Air Partnership (Air Sciences, 2005). Soil NO$_x$ emissions, including emissions from fertilizer application, are computed according to Hudman et al. (2012), with a 50 % reduction in the midwestern US for summertime based on a previous comparison with OMI NO$_2$ observations (Vinken et al., 2014). Lightning NO$_x$ emissions are described by Murray et al. (2012) with a horizontal distribution matching climatological observations of lightning flashes, interannual variability driven by MERRA-2 convection, and most of the release at the top of convective updrafts (Ott et al., 2010). The NO$_x$ yield per flash is 260 mol to the south of 35° N and 500 mol to the north (Hudman et al., 2007; Huntrieser et al., 2008, 2009; Ott et al., 2010; Travis et al., 2016).

The GEOS-Chem simulation of NO$_x$ and related species over the US has been evaluated in a number of recent papers including Zhang et al. (2012), Ellis et al. (2013), and Lee et al. (2016) for nitrogen deposition; Travis et al. (2016) for NO$_x$ concentrations over the southeastern US during the SEAC[4]RS campaign; Fisher et al. (2016) for organic nitrates during that same campaign; Jaeglé et al. (2018) for the WINTER campaign; and Fischer et al. (2014) for the ensemble of PAN observations. These evaluations find that the model is overall successful with no indication of systematic bias.

References

Air Sciences: 2002 Fire Emission Inventory for the WRAP Region – Phase II, Denver and Portland, 2005.

Amedro, D., Bunkan, A. J. C., Berasategui, M., and Crowley, J. N.: Kinetics of the OH+NO$_2$ reaction: Rate coefficients (217–333 K, 16–1200 mbar) and fall-off parameters for N$_2$ and O$_2$ bath-gases, Atmos. Chem. Phys. Discuss., https://doi.org/10.5194/acp-2019-297, in review, 2019.

Anderson, D. C., Loughner, C. P., Diskin, G., Weinheimer, A., Canty, T. P., Salawitch, R. J., Worden, H. M., Fried, A., Mikoviny, T., Wisthaler, A., and Dickerson, R. R.: Measured and modeled CO and NO$_y$ in DISCOVER-AQ: An evaluation of emissions and chemistry over the eastern US, Atmos. Environ., 96, 78–87, https://doi.org/10.1016/j.atmosenv.2014.07.004, 2014.

Anderson, J. G., Weisenstein, D. K., Bowman, K. P., Homeyer, C. R., Smith, J. B., Wilmouth, D. M., Sayres, D. S., Klobas, J. E., Leroy, S. S., Dykema, J. A., and Wofsy, S. C.: Stratospheric ozone over the United States in summer linked to observations of convection and temperature via chlorine and bromine catalysis, P. Natl. Acad. Sci. USA, 114, E4905–E4913, https://doi.org/10.1073/pnas.1619318114, 2017.

Anderson, J. G., Clapp, C. E., Bowman, K. P., Homeyer, C. R., Weisenstein, D. K., Smith, J. B., Wilmouth, D. M., and Klobas, J. E.: Coupling Free Radical Catalysis, Convective Injection into the Stratosphere, Climate Forcing, and Human Health, AMS Annual Meeting, Phoenix, AZ, 2019.

Astitha, M., Luo, H. Y., Rao, S. T., Hogrefe, C., Mathur, R., and Kumar, N.: Dynamic evaluation of two decades of WRF-CMAQ ozone simulations over the contiguous United States, Atmos. Environ., 164, 102–116, https://doi.org/10.1016/j.atmosenv.2017.05.020, 2017.

Bedka, K., Murillo, E. M., Homeyer, C. R., Scarino, B., and Mersiovsky, H.: The Above-Anvil Cirrus Plume: An Important Severe Weather Indicator in Visible and Infrared Satelite Imagery, Weather Forecast., 33, 1159–1181, https://doi.org/10.1175/waf-d-18-0040.1, 2018.

Belmonte Rivas, M., Veefkind, P., Eskes, H., and Levelt, P.: OMI tropospheric NO$_2$ profiles from cloud slicing: constraints on surface emissions, convective transport and lightning NO$_x$, Atmos. Chem. Phys., 15, 13519–13553, https://doi.org/10.5194/acp-15-13519-2015, 2015.

Blanchard, C. L. and Hidy, G. M.: Ozone response to emission reductions in the southeastern United States, Atmos. Chem. Phys., 18, 8183–8202, https://doi.org/10.5194/acp-18-8183-2018, 2018.

Boersma, K. F., Jacob, D. J., Bucsela, E. J., Perring, A. E., Dirksen, R., van der A, R. J., Yantosca, R. M., Park, R. J., Wenig, M. O., Bertram, T. H., and Cohen, R. C.: Validation of OMI tropospheric NO$_2$ observations during INTEX-B and application to constrain NO$_x$ emissions over the eastern United States and Mexico, Atmos. Environ., 42, 4480–4497, https://doi.org/10.1016/j.atmosenv.2008.02.004, 2008.

Boersma, K. F., Eskes, H. J., Dirksen, R. J., van der A, R. J., Veefkind, J. P., Stammes, P., Huijnen, V., Kleipool, Q. L., Sneep, M., Claas, J., Leitão, J., Richter, A., Zhou, Y., and Brunner, D.: An improved tropospheric NO$_2$ column retrieval algorithm for the Ozone Monitoring Instrument, Atmos. Meas. Tech., 4, 1905–1928, https://doi.org/10.5194/amt-4-1905-2011, 2011.

Brioude, J., Angevine, W. M., Ahmadov, R., Kim, S.-W., Evan, S., McKeen, S. A., Hsie, E.-Y., Frost, G. J., Neuman, J. A., Pollack, I. B., Peischl, J., Ryerson, T. B., Holloway, J., Brown, S. S., Nowak, J. B., Roberts, J. M., Wofsy, S. C., Santoni, G. W., Oda, T., and Trainer, M.: Top-down estimate of surface flux in the Los Angeles Basin using a mesoscale inverse modeling technique: assessing anthropogenic emissions of CO, NO$_x$ and CO$_2$ and their impacts, Atmos. Chem. Phys., 13, 3661–3677, https://doi.org/10.5194/acp-13-3661-2013, 2013.

Bucsela, E. J., Krotkov, N. A., Celarier, E. A., Lamsal, L. N., Swartz, W. H., Bhartia, P. K., Boersma, K. F., Veefkind, J. P., Gleason, J. F., and Pickering, K. E.: A new stratospheric and tropospheric NO$_2$ retrieval algorithm for nadir-viewing satellite instruments: applications to OMI, Atmos. Meas. Tech., 6, 2607–2626, https://doi.org/10.5194/amt-6-2607-2013, 2013.

Castellanos, P., Marufu, L. T., Doddridge, B. G., Taubman, B. F., Schwab, J. J., Hains, J. C., Ehrman, S. H., and Dickerson, R. R.: Ozone, oxides of nitrogen, and carbon monoxide during pollution events over the eastern United States: An evaluation of emissions and vertical mixing, J. Geophys. Res.-Atmos., 116, D16307, https://doi.org/10.1029/2010jd014540, 2011.

Chang, K. L., Petropavlovskikh, I., Cooper, O. R., Schultz, M. G., and Wang, T.: Regional trend analysis of surface ozone observations from monitoring networks in eastern North America, Europe and East Asia, Elementa-Sci. Anthrop., 5, 22, https://doi.org/10.1525/elementa.243, 2017.

Choi, S., Joiner, J., Choi, Y., Duncan, B. N., Vasilkov, A., Krotkov, N., and Bucsela, E.: First estimates of global free-tropospheric NO$_2$ abundances derived using a cloud-slicing technique applied to satellite observations from the Aura Ozone Monitoring Instrument (OMI), Atmos. Chem. Phys., 14, 10565–10588, https://doi.org/10.5194/acp-14-10565-2014, 2014.

Cooney, J. W., Bowman, K. P., Homeyer, C. R., and Fenske, T. M.: Ten Year Analysis of Tropopause-Overshooting Convection Using GridRad Data, J. Geophys. Res.-Atmos., 123, 329–343, https://doi.org/10.1002/2017jd027718, 2018.

Cooper, O. R., Oltmans, S. J., Johnson, B. J., Brioude, J., Angevine, W., Trainer, M., Parrish, D. D., Ryerson, T. R., Pollack, I., Cullis, P. D., Ives, M. A., Tarasick, D. W., Al-Saadi, J., and Stajner, I.: Measurement of western US baseline ozone from the surface to the tropopause and assessment of downwind impact regions, J. Geophys. Res.-Atmos., 116, D00V03, https://doi.org/10.1029/2011jd016095, 2011.

Dallmann, T. R. and Harley, R. A.: Evaluation of mobile source emission trends in the United States, J. Geophys. Res.-Atmos., 115, D14305, https://doi.org/10.1029/2010jd013862, 2010.

Darmenov, A. and da Silva, A. M.: The Quick Fire Emissions Dataset (QFED) – Documentation of versions 2.1, 2.2 and 2.4, NASA, Greenbelt, MD, 183 pp., 2013.

Day, D. A., Wooldridge, P. J., Dillon, M. B., Thornton, J. A., and Cohen, R. C.: A thermal dissociation laser-induced fluorescence instrument for in situ detection of NO$_2$, peroxy nitrates, alkyl nitrates, and HNO$_3$, J. Geophys. Res.-Atmos., 107, ACH 4-1–ACH 4-14, https://doi.org/10.1029/2001jd000779, 2002.

de Foy, B., Lu, Z. F., Streets, D. G., Lamsal, L. N., and Duncan, B. N.: Estimates of power plant NO$_x$ emissions and lifetimes from OMI NO$_2$ satellite retrievals, Atmos. Environ., 116, 1–11, https://doi.org/10.1016/j.atmosenv.2015.05.056, 2015.

de Foy, B., Lu, Z. F., and Streets, D. G.: Impacts of control strategies, the Great Recession and weekday variations on NO$_2$ columns above North American cities, Atmos. Environ., 138, 74–86, https://doi.org/10.1016/j.atmosenv.2016.04.038, 2016.

Demerjian, K. L.: A review of national monitoring networks in North America, Atmos. Environ., 34, 1861–1884, https://doi.org/10.1016/s1352-2310(99)00452-5, 2000.

Di Luzio, M., Johnson, G. L., Daly, C., Eischeid, J. K., and Arnold, J. G.: Constructing retrospective gridded daily precipitation and temperature datasets for the conterminous United States, J. Appl. Meteorol. Clim., 47, 475–497, https://doi.org/10.1175/2007jamc1356.1, 2008.

Dobber, M., Voors, R., Dirksen, R., Kleipool, Q., and Levelt, P.: The high-resolution solar reference spectrum between 250 and 550 nm and its application to measurements with the Ozone Monitoring Instrument, Sol. Phys., 249, 281–291, https://doi.org/10.1007/s11207-008-9187-7, 2008.

Duncan, B. N., Yoshida, Y., de Foy, B., Lamsal, L. N., Streets, D. G., Lu, Z. F., Pickering, K. E., and Krotkov, N. A.: The observed response of Ozone Monitoring Instrument (OMI) NO$_2$ columns to NO$_x$ emission controls on power plants in the United States: 2005–2011, Atmos. Environ., 81, 102–111, https://doi.org/10.1016/j.atmosenv.2013.08.068, 2013.

Duncan, B. N., Lamsal, L. N., Thompson, A. M., Yoshida, Y., Lu, Z. F., Streets, D. G., Hurwitz, M. M., and Pickering, K. E.: A space-based, high-resolution view of notable changes in urban NO$_x$ pollution around the world (2005–2014), J. Geophys. Res.-

Atmos., 121, 976–996, https://doi.org/10.1002/2015jd024121, 2016.

Dunlea, E. J., Herndon, S. C., Nelson, D. D., Volkamer, R. M., San Martini, F., Sheehy, P. M., Zahniser, M. S., Shorter, J. H., Wormhoudt, J. C., Lamb, B. K., Allwine, E. J., Gaffney, J. S., Marley, N. A., Grutter, M., Marquez, C., Blanco, S., Cardenas, B., Retama, A., Ramos Villegas, C. R., Kolb, C. E., Molina, L. T., and Molina, M. J.: Evaluation of nitrogen dioxide chemiluminescence monitors in a polluted urban environment, Atmos. Chem. Phys., 7, 2691–2704, https://doi.org/10.5194/acp-7-2691-2007, 2007.

Edgerton, E. S., Hartsell, B. E., Saylor, R. D., Jansen, J. J., Hansen, D. A., and Hidy, G. M.: The Southeastern Aerosol Research and Characterization Study, part 3: Continuous measurements of fine particulate matter mass and composition, J. Air Waste Manage., 56, 1325–1341, https://doi.org/10.1080/10473289.2006.10464585, 2006.

Ellis, R. A., Jacob, D. J., Sulprizio, M. P., Zhang, L., Holmes, C. D., Schichtel, B. A., Blett, T., Porter, E., Pardo, L. H., and Lynch, J. A.: Present and future nitrogen deposition to national parks in the United States: critical load exceedances, Atmos. Chem. Phys., 13, 9083–9095, https://doi.org/10.5194/acp-13-9083-2013, 2013.

EPA: Annual Average Emissions, Air Pollutant Emission Trends Data, available at: https://www.epa.gov/air-emissions-inventories/air-pollutant-emissions-trends-data, last access: 23 July 2018.

Fiore, A. M., Naik, V., and Leibensperger, E. M.: Air Quality and Climate Connections, J. Air Waste Manage., 65, 645–685, https://doi.org/10.1080/10962247.2015.1040526, 2015.

Fischer, E. V., Jacob, D. J., Yantosca, R. M., Sulprizio, M. P., Millet, D. B., Mao, J., Paulot, F., Singh, H. B., Roiger, A., Ries, L., Talbot, R. W., Dzepina, K., and Pandey Deolal, S.: Atmospheric peroxyacetyl nitrate (PAN): a global budget and source attribution, Atmos. Chem. Phys., 14, 2679–2698, https://doi.org/10.5194/acp-14-2679-2014, 2014.

Fisher, J. A., Jacob, D. J., Travis, K. R., Kim, P. S., Marais, E. A., Chan Miller, C., Yu, K., Zhu, L., Yantosca, R. M., Sulprizio, M. P., Mao, J., Wennberg, P. O., Crounse, J. D., Teng, A. P., Nguyen, T. B., St. Clair, J. M., Cohen, R. C., Romer, P., Nault, B. A., Wooldridge, P. J., Jimenez, J. L., Campuzano-Jost, P., Day, D. A., Hu, W., Shepson, P. B., Xiong, F., Blake, D. R., Goldstein, A. H., Misztal, P. K., Hanisco, T. F., Wolfe, G. M., Ryerson, T. B., Wisthaler, A., and Mikoviny, T.: Organic nitrate chemistry and its implications for nitrogen budgets in an isoprene- and monoterpene-rich atmosphere: constraints from aircraft (SEAC^{4}RS) and ground-based (SOAS) observations in the Southeast US, Atmos. Chem. Phys., 16, 5969–5991, https://doi.org/10.5194/acp-16-5969-2016, 2016.

Fisher, J. A., Atlas, E. L., Barletta, B., Meinardi, S., Blake, D. R., Thompson, C. R., Ryerson, T. B., Peischl, J., Tzompa-Sosa, Z. A., and Murray, L. T.: Methyl, Ethyl, and Propyl Nitrates: Global Distribution and Impacts on Reactive Nitrogen in Remote Marine Environments, J. Geophys. Res.-Atmos., 123, 12429–12451, https://doi.org/10.1029/2018jd029046, 2018.

Fujita, E. M., Campbell, D. E., Zielinska, B., Chow, J. C., Lindhjem, C. E., DenBleyker, A., Bishop, G. A., Schuchmann, B. G., Stedman, D. H., and Lawson, D. R.: Comparison of the MOVES2010a, MOBILE6.2, and EMFAC2007 mobile source

emission models with on-road traffic tunnel and remote sensing measurements, J. Air Waste Manage., 62, 1134–1149, https://doi.org/10.1080/10962247.2012.699016, 2012.

Gelaro, R., McCarty, W., Suarez, M. J., Todling, R., Molod, A., Takacs, L., Randles, C. A., Darmenov, A., Bosilovich, M. G., Reichle, R., Wargan, K., Coy, L., Cullather, R., Draper, C., Akella, S., Buchard, V., Conaty, A., da Silva, A. M., Gu, W., Kim, G. K., Koster, R., Lucchesi, R., Merkova, D., Nielsen, J. E., Partyka, G., Pawson, S., Putman, W., Rienecker, M., Schubert, S. D., Sienkiewicz, M., and Zhao, B.: The Modern-Era Retrospective Analysis for Research and Applications, Version 2 (MERRA-2), J. Climate, 30, 5419–5454, https://doi.org/10.1175/jcli-d-16-0758.1, 2017.

Goldberg, D. L., Vinciguerra, T. P., Anderson, D. C., Hembeck, L., Canty, T. P., Ehrman, S. H., Martins, D. K., Stauffer, R. M., Thompson, A. M., Salawitch, R. J., and Dickerson, R. R.: CAMx ozone source attribution in the eastern United States using guidance from observations during DISCOVER-AQ Maryland, Geophys. Res. Lett., 43, 2249–2258, https://doi.org/10.1002/2015gl067332, 2016.

Hansen, D. A., Edgerton, E. S., Hartsell, B. E., Jansen, J. J., Kandasamy, N., Hidy, G. M., and Blanchard, C. L.: The southeastern aerosol research and characterization study: Part 1-overview, J. Air Waste Manage., 53, 1460–1471, https://doi.org/10.1080/10473289.2003.10466318, 2003.

Herman, R. L., Ray, E. A., Rosenlof, K. H., Bedka, K. M., Schwartz, M. J., Read, W. G., Troy, R. F., Chin, K., Christensen, L. E., Fu, D., Stachnik, R. A., Bui, T. P., and Dean-Day, J. M.: Enhanced stratospheric water vapor over the summertime continental United States and the role of overshooting convection, Atmos. Chem. Phys., 17, 6113–6124, https://doi.org/10.5194/acp-17-6113-2017, 2017.

Hidy, G. M. and Blanchard, C. L.: Precursor reductions and ground-level ozone in the Continental United States, J. Air Waste Manage., 65, 1261–1282, https://doi.org/10.1080/10962247.2015.1079564, 2015.

Hudman, R. C., Jacob, D. J., Turquety, S., Leibensperger, E. M., Murray, L. T., Wu, S., Gilliland, A. B., Avery, M., Bertram, T. H., Brune, W., Cohen, R. C., Dibb, J. E., Flocke, F. M., Fried, A., Holloway, J., Neuman, J. A., Orville, R., Perring, A., Ren, X., Sachse, G. W., Singh, H. B., Swanson, A., and Wooldridge, P. J.: Surface and lightning sources of nitrogen oxides over the United States: Magnitudes, chemical evolution, and outflow, J. Geophys. Res.-Atmos., 112, D12S05, https://doi.org/10.1029/2006jd007912, 2007.

Hudman, R. C., Moore, N. E., Mebust, A. K., Martin, R. V., Russell, A. R., Valin, L. C., and Cohen, R. C.: Steps towards a mechanistic model of global soil nitric oxide emissions: implementation and space based-constraints, Atmos. Chem. Phys., 12, 7779–7795, https://doi.org/10.5194/acp-12-7779-2012, 2012.

Huntrieser, H., Schumann, U., Schlager, H., Höller, H., Giez, A., Betz, H.-D., Brunner, D., Forster, C., Pinto Jr., O., and Calheiros, R.: Lightning activity in Brazilian thunderstorms during TROC-CINOX: implications for NOx production, Atmos. Chem. Phys., 8, 921–953, https://doi.org/10.5194/acp-8-921-2008, 2008.

Huntrieser, H., Schlager, H., Lichtenstern, M., Roiger, A., Stock, P., Minikin, A., Höller, H., Schmidt, K., Betz, H.-D., Allen, G., Viciani, S., Ulanovsky, A., Ravegnani, F., and Brunner, D.: NO$_x$ production by lightning in Hector: first airborne measurements during SCOUT-O3/ACTIVE, Atmos. Chem. Phys., 9, 8377–8412, https://doi.org/10.5194/acp-9-8377-2009, 2009.

Huntrieser, H., Lichtenstern, M., Scheibe, M., Aufmhoff, H., Schlager, H., Pucik, T., Minikin, A., Weinzierl, B., Heimerl, K., Futterer, D., Rappengluck, B., Ackermann, L., Pickering, K. E., Cummings, K. A., Biggerstaff, M. I., Betten, D. P., Honomichl, S., and Barth, M. C.: On the origin of pronounced O$_3$ gradients in the thunderstorm outflow region during DC3, J. Geophys. Res.-Atmos., 121, 6600–6637, https://doi.org/10.1002/2015jd024279, 2016a.

Huntrieser, H., Lichtenstern, M., Scheibe, M., Aufmhoff, H., Schlager, H., Pucik, T., Minikin, A., Weinzierl, B., Heimerl, K., Pollack, I. B., Peischl, J., Ryerson, T. B., Weinheimer, A. J., Honomichl, S., Ridley, B. A., Biggerstaff, M. I., Betten, D. P., Hair, J. W., Butler, C. F., Schwartz, M. J., and Barth, M. C.: Injection of lightning-produced NO$_x$, water vapor, wildfire emissions, and stratospheric air to the UT/LS as observed from DC3 measurements, J. Geophys. Res.-Atmos., 121, 6638–6668, https://doi.org/10.1002/2015jd024273, 2016b.

Jaeglé, L., Shah, V., Thornton, J. A., Lopez-Hilfiker, F. D., Lee, B. H., McDuffie, E. E., Fibiger, D., Brown, S. S., Veres, P., Sparks, T. L., Ebben, C. J., Wooldridge, P. J., Kenagy, H. S., Cohen, R. C., Weinheimer, A. J., Campos, T. L., Montzka, D. D., Digangi, J. P., Wolfe, G. M., Hanisco, T., Schroder, J. C., Campuzano-Jost, P., Day, D. A., Jimenez, J. L., Sullivan, A. P., Guo, H., and Weber, R. J.: Nitrogen Oxides Emissions, Chemistry, Deposition, and Export Over the Northeast United States During the WINTER Aircraft Campaign, J. Geophys. Res.-Atmos., 123, 12368–12393, https://doi.org/10.1029/2018jd029133, 2018.

Jaffe, D. A., Cooper, O. R., Fiore, A. M., Henderson, B. H., Tonnesen, G. S., Russell, A. G., Henze, D. K., Langford, A. O., Lin, M. Y., and Moore, T.: Scientific assessment of background ozone over the US: Implications for air quality management, Elementa-Sci. Anthrop., 6, 30, https://doi.org/10.1525/elementa.309, 2018.

Jia, L. W., Vecchi, G. A., Yang, X. S., Gudgel, R. G., Delworth, T. L., Stern, W. F., Paffendorf, K., Underwood, S. D., and Zeng, F. R.: The Roles of Radiative Forcing, Sea Surface Temperatures, and Atmospheric and Land Initial Conditions in US Summer Warming Episodes, J. Climate, 29, 4121–4135, https://doi.org/10.1175/jcli-d-15-0471.1, 2016.

Jiang, Z., McDonald, B. C., Worden, H., Worden, J. R., Miyazaki, K., Qu, Z., Henze, D. K., Jones, D. B. A., Arellano, A. F., Fischer, E. V., Zhu, L. Y., and Boersma, K. F.: Unexpected slowdown of US pollutant emission reduction in the past decade, P. Natl. Acad. Sci. USA, 115, 5099–5104, https://doi.org/10.1073/pnas.1801191115, 2018.

Kenagy, H. S., Sparks, T. L., Ebben, C. J., Wooldrige, P. J., Lopez-Hilfiker, F. D., Lee, B. H., Thornton, J. A., McDuffie, E. E., Fibiger, D. L., Brown, S. S., Montzka, D. D., Weinheimer, A. J., Schroder, J. C., Campuzano-Jost, P., Day, D. A., Jimenez, J. L., Dibb, J. E., Campos, T., Shah, V., Jaegle, L., and Cohen, R. C.: NO$_x$ Lifetime and NO$_y$ Partitioning During WINTER, J. Geophys. Res.-Atmos., 123, 9813–9827, https://doi.org/10.1029/2018jd028736, 2018.

Kharol, S. K., Martin, R. V., Philip, S., Boys, B., Lamsal, L. N., Jerrett, M., Brauer, M., Crouse, D. L., McLinden, C., and Burnett, R. T.: Assessment of the magnitude and recent trends in satellite-derived ground-level nitrogen diox-

ide over North America, Atmos. Environ., 118, 236–245, https://doi.org/10.1016/j.atmosenv.2015.08.011, 2015.

Kim, S. W., McDonald, B. C., Baidar, S., Brown, S. S., Dube, B., Ferrare, R. A., Frost, G. J., Harley, R. A., Holloway, J. S., Lee, H. J., McKeen, S. A., Neuman, J. A., Nowak, J. B., Oetjen, H., Ortega, I., Pollack, I. B., Roberts, J. M., Ryerson, T. B., Scarino, A. J., Senff, C. J., Thalman, R., Trainer, M., Volkamer, R., Wagner, N., Washenfelder, R. A., Waxman, E., and Young, C. J.: Modeling the weekly cycle of NO_x and CO emissions and their impacts on O_3 in the Los Angeles-South Coast Air Basin during the CalNex 2010 field campaign, J. Geophys. Res.-Atmos., 121, 1340–1360, https://doi.org/10.1002/2015jd024292, 2016.

Kleipool, Q. L., Dobber, M. R., de Haan, J. F., and Levelt, P. F.: Earth surface reflectance climatology from 3 years of OMI data, J. Geophys. Res.-Atmos., 113, D18308, https://doi.org/10.1029/2008jd010290, 2008.

Koshak, W. J., Cummins, K. L., Buechler, D. E., Vant-Hull, B., Blakeslee, R. J., Williams, E. R., and Peterson, H. S.: Variability of CONUS Lightning in 2003–12 and Associated Impacts, J. Appl. Meteorol. Clim., 54, 15–41, https://doi.org/10.1175/jamc-d-14-0072.1, 2015.

Krotkov, N. A., McLinden, C. A., Li, C., Lamsal, L. N., Celarier, E. A., Marchenko, S. V., Swartz, W. H., Bucsela, E. J., Joiner, J., Duncan, B. N., Boersma, K. F., Veefkind, J. P., Levelt, P. F., Fioletov, V. E., Dickerson, R. R., He, H., Lu, Z., and Streets, D. G.: Aura OMI observations of regional SO_2 and NO_2 pollution changes from 2005 to 2015, Atmos. Chem. Phys., 16, 4605–4629, https://doi.org/10.5194/acp-16-4605-2016, 2016.

Krotkov, N. A., Lamsal, L. N., Celarier, E. A., Swartz, W. H., Marchenko, S. V., Bucsela, E. J., Chan, K. L., Wenig, M., and Zara, M.: The version 3 OMI NO_2 standard product, Atmos. Meas. Tech., 10, 3133–3149, https://doi.org/10.5194/amt-10-3133-2017, 2017.

Kuang, S., Newchurch, M. J., Thompson, A. M., Stauffer, R. M., Johnson, B. J., and Wang, L. H.: Ozone Variability and Anomalies Observed During SENEX and SEAC⁴RS Campaigns in 2013, J. Geophys. Res.-Atmos., 122, 11227–11241, https://doi.org/10.1002/2017jd027139, 2017.

Lamsal, L. N., Martin, R. V., van Donkelaar, A., Steinbacher, M., Celarier, E. A., Bucsela, E., Dunlea, E. J., and Pinto, J. P.: Ground-level nitrogen dioxide concentrations inferred from the satellite-borne Ozone Monitoring Instrument, J. Geophys. Res.-Atmos., 113, D16308, https://doi.org/10.1029/2007jd009235, 2008.

Lamsal, L. N., Krotkov, N. A., Celarier, E. A., Swartz, W. H., Pickering, K. E., Bucsela, E. J., Gleason, J. F., Martin, R. V., Philip, S., Irie, H., Cede, A., Herman, J., Weinheimer, A., Szykman, J. J., and Knepp, T. N.: Evaluation of OMI operational standard NO_2 column retrievals using in situ and surface-based NO_2 observations, Atmos. Chem. Phys., 14, 11587–11609, https://doi.org/10.5194/acp-14-11587-2014, 2014.

Lamsal, L. N., Duncan, B. N., Yoshida, Y., Krotkov, N. A., Pickering, K. E., Streets, D. G., and Lu, Z. F.: U.S. NO_2 trends (2005–2013): EPA Air Quality System (AQS) data versus improved observations from the Ozone Monitoring Instrument (OMI), Atmos. Environ., 110, 130–143, https://doi.org/10.1016/j.atmosenv.2015.03.055, 2015.

Laughner, J. L.: Space-based constraints on NO_x lifetime using high-resolution NO_2 retrievals, Department of Chemistry, University of California, Berkeley, 2018.

Laughner, J. L. and Cohen, R. C.: Direct space-based observation of decadal changes in NO_x emissions and lifetime: implications for oxidative capacity, AGU Fall Meeting, Washington, D.C., 2018.

Laughner, J. L., Zhu, Q., and Cohen, R. C.: The Berkeley High Resolution Tropospheric NO_2 product, Earth Syst. Sci. Data, 10, 2069–2095, https://doi.org/10.5194/essd-10-2069-2018, 2018.

Lee, H.-M., Paulot, F., Henze, D. K., Travis, K., Jacob, D. J., Pardo, L. H., and Schichtel, B. A.: Sources of nitrogen deposition in Federal Class I areas in the US, Atmos. Chem. Phys., 16, 525–540, https://doi.org/10.5194/acp-16-525-2016, 2016.

Leue, C., Wenig, M., Wagner, T., Klimm, O., Platt, U., and Jahne, B.: Quantitative analysis of NO_x emissions from Global Ozone Monitoring Experiment satellite image sequences, J. Geophys. Res.-Atmos., 106, 5493–5505, https://doi.org/10.1029/2000jd900572, 2001.

Levelt, P. F., Van den Oord, G. H. J., Dobber, M. R., Malkki, A., Visser, H., de Vries, J., Stammes, P., Lundell, J. O. V., and Saari, H.: The Ozone Monitoring Instrument, IEEE T. Geosci. Remote Sens., 44, 1093–1101, https://doi.org/10.1109/tgrs.2006.872333, 2006.

Levelt, P. F., Joiner, J., Tamminen, J., Veefkind, J. P., Bhartia, P. K., Stein Zweers, D. C., Duncan, B. N., Streets, D. G., Eskes, H., van der A, R., McLinden, C., Fioletov, V., Carn, S., de Laat, J., DeLand, M., Marchenko, S., McPeters, R., Ziemke, J., Fu, D., Liu, X., Pickering, K., Apituley, A., González Abad, G., Arola, A., Boersma, F., Chan Miller, C., Chance, K., de Graaf, M., Hakkarainen, J., Hassinen, S., Ialongo, I., Kleipool, Q., Krotkov, N., Li, C., Lamsal, L., Newman, P., Nowlan, C., Suleiman, R., Tilstra, L. G., Torres, O., Wang, H., and Wargan, K.: The Ozone Monitoring Instrument: overview of 14 years in space, Atmos. Chem. Phys., 18, 5699–5745, https://doi.org/10.5194/acp-18-5699-2018, 2018.

Li, J., Mao, J., Fiore, A. M., Cohen, R. C., Crounse, J. D., Teng, A. P., Wennberg, P. O., Lee, B. H., Lopez-Hilfiker, F. D., Thornton, J. A., Peischl, J., Pollack, I. B., Ryerson, T. B., Veres, P., Roberts, J. M., Neuman, J. A., Nowak, J. B., Wolfe, G. M., Hanisco, T. F., Fried, A., Singh, H. B., Dibb, J., Paulot, F., and Horowitz, L. W.: Decadal changes in summertime reactive oxidized nitrogen and surface ozone over the Southeast United States, Atmos. Chem. Phys., 18, 2341–2361, https://doi.org/10.5194/acp-18-2341-2018, 2018.

Lin, M., Horowitz, L. W., Payton, R., Fiore, A. M., and Tonnesen, G.: US surface ozone trends and extremes from 1980 to 2014: quantifying the roles of rising Asian emissions, domestic controls, wildfires, and climate, Atmos. Chem. Phys., 17, 2943–2970, https://doi.org/10.5194/acp-17-2943-2017, 2017.

Lorente, A., Folkert Boersma, K., Yu, H., Dörner, S., Hilboll, A., Richter, A., Liu, M., Lamsal, L. N., Barkley, M., De Smedt, I., Van Roozendael, M., Wang, Y., Wagner, T., Beirle, S., Lin, J.-T., Krotkov, N., Stammes, P., Wang, P., Eskes, H. J., and Krol, M.: Structural uncertainty in air mass factor calculation for NO_2 and HCHO satellite retrievals, Atmos. Meas. Tech., 10, 759–782, https://doi.org/10.5194/amt-10-759-2017, 2017.

Lu, Z., Streets, D. G., de Foy, B., Lamsal, L. N., Duncan, B. N., and Xing, J.: Emissions of nitrogen oxides from US urban areas: estimation from Ozone Monitoring Instrument re-

trievals for 2005–2014, Atmos. Chem. Phys., 15, 10367–10383, https://doi.org/10.5194/acp-15-10367-2015, 2015.

Marais, E. A., Jacob, D. J., Jimenez, J. L., Campuzano-Jost, P., Day, D. A., Hu, W., Krechmer, J., Zhu, L., Kim, P. S., Miller, C. C., Fisher, J. A., Travis, K., Yu, K., Hanisco, T. F., Wolfe, G. M., Arkinson, H. L., Pye, H. O. T., Froyd, K. D., Liao, J., and McNeill, V. F.: Aqueous-phase mechanism for secondary organic aerosol formation from isoprene: application to the southeast United States and co-benefit of SO$_2$ emission controls, Atmos. Chem. Phys., 16, 1603–1618, https://doi.org/10.5194/acp-16-1603-2016, 2016.

Marais, E. A., Jacob, D. J., Choi, S., Joiner, J., Belmonte-Rivas, M., Cohen, R. C., Beirle, S., Murray, L. T., Schiferl, L. D., Shah, V., and Jaeglé, L.: Nitrogen oxides in the global upper troposphere: interpreting cloud-sliced NO$_2$ observations from the OMI satellite instrument, Atmos. Chem. Phys., 18, 17017–17027, https://doi.org/10.5194/acp-18-17017-2018, 2018.

Martin, R. V., Chance, K., Jacob, D. J., Kurosu, T. P., Spurr, R. J. D., Bucsela, E., Gleason, J. F., Palmer, P. I., Bey, I., Fiore, A. M., Li, Q. B., Yantosca, R. M., and Koelemeijer, R. B. A.: An improved retrieval of tropospheric nitrogen dioxide from GOME, J. Geophys. Res.-Atmos., 107, ACH 9-1–ACH 9-21 https://doi.org/10.1029/2001jd001027, 2002.

Martin, R. V., Jacob, D. J., Chance, K., Kurosu, T. P., Palmer, P. I., and Evans, M. J.: Global inventory of nitrogen oxide emissions constrained by space-based observations of NO$_2$ columns, J. Geophys. Res.-Atmos., 108, 4537, https://doi.org/10.1029/2003jd003453, 2003.

McDonald, B. C., Gentner, D. R., Goldstein, A. H., and Harley, R. A.: Long-Term Trends in Motor Vehicle Emissions in US Urban Areas, Environ. Sci. Technol., 47, 10022–10031, https://doi.org/10.1021/es401034z, 2012.

McDonald, B. C., McKeen, S. A., Cui, Y. Y., Ahmadov, R., Kim, S. W., Frost, G. J., Pollack, I. B., Peischl, J., Ryerson, T. B., Holloway, J. S., Graus, M., Wameke, C., Gilman, J. B., de Gouw, J. A., Kaiser, J., Keutsch, F. N., Hanisco, T. F., Wolfe, G. M., and Trainer, M.: Modeling Ozone in the Eastern US using a Fuel-Based Mobile Source Emissions Inventory, Environ. Sci. Technol., 52, 7360–7370, https://doi.org/10.1021/acs.est.8b00778, 2018.

McDuffie, E. E., Fibiger, D. L., Dube, W. P., Lopez-Hilfiker, F., Lee, B. H., Thornton, J. A., Shah, V., Jaegle, L., Guo, H. Y., Weber, R. J., Reeves, J. M., Weinheimer, A. J., Schroder, J. C., Campuzano-Jost, P., Jimenez, J. L., Dibb, J. E., Veres, P., Ebben, C., Sparks, T. L., Wooldridge, P. J., Cohen, R. C., Hornbrook, R. S., Apel, E. C., Campos, T., Hall, S. R., Ullmann, K., and Brown, S. S.: Heterogeneous N$_2$O$_5$ Uptake During Winter: Aircraft Measurements During the 2015 WINTER Campaign and Critical Evaluation of Current Parameterizations, J. Geophys. Res.-Atmos., 123, 4345–4372, https://doi.org/10.1002/2018jd028336, 2018.

Murray, L. T., Jacob, D. J., Logan, J. A., Hudman, R. C., and Koshak, W. J.: Optimized regional and interannual variability of lightning in a global chemical transport model constrained by LIS/OTD satellite data, J. Geophys. Res.-Atmos., 117, D20307, https://doi.org/10.1029/2012jd017934, 2012.

Nault, B. A., Garland, C., Pusede, S. E., Wooldridge, P. J., Ullmann, K., Hall, S. R., and Cohen, R. C.: Measurements of CH$_3$O$_2$NO$_2$ in the upper troposphere, Atmos. Meas. Tech., 8, 987–997, https://doi.org/10.5194/amt-8-987-2015, 2015.

Ott, L. E., Pickering, K. E., Stenchikov, G. L., Allen, D. J., DeCaria, A. J., Ridley, B., Lin, R. F., Lang, S., and Tao, W. K.: Production of lightning NO$_x$ and its vertical distribution calculated from three-dimensional cloud-scale chemical transport model simulations, J. Geophys. Res.-Atmos., 115, D04301, https://doi.org/10.1029/2009jd011880, 2010.

Palmer, P. I., Jacob, D. J., Chance, K., Martin, R. V., Spurr, R. J. D., Kurosu, T. P., Bey, I., Yantosca, R., Fiore, A., and Li, Q. B.: Air mass factor formulation for spectroscopic measurements from satellites: Application to formaldehyde retrievals from the Global Ozone Monitoring Experiment, J. Geophys. Res.-Atmos., 106, 14539–14550, https://doi.org/10.1029/2000jd900772, 2001.

Paulot, F., Jacob, D. J., Pinder, R. W., Bash, J. O., Travis, K., and Henze, D. K.: Ammonia emissions in the United States, European Union, and China derived by high-resolution inversion of ammonium wet deposition data: Interpretation with a new agricultural emissions inventory (MASAGE_NH3), J. Geophys. Res.-Atmos., 119, 4343–4364, https://doi.org/10.1002/2013jd021130, 2014.

Pollack, I. B., Lerner, B. M., and Ryerson, T. B.: Evaluation of ultra-violet light-emitting diodes for detection of atmospheric NO$_2$ by photolysis-chemiluminescence, J. Atmos. Chem., 65, 111–125, https://doi.org/10.1007/s10874-011-9184-3, 2010.

Randel, W. J., Moyer, E., Park, M., Jensen, E., Bernath, P., Walker, K., and Boone, C.: Global variations of HDO and HDO/H$_2$O ratios in the upper troposphere and lower stratosphere derived from ACE-FTS satellite measurements, J. Geophys. Res.-Atmos., 117, D06303, https://doi.org/10.1029/2011jd016632, 2012.

Reed, C., Evans, M. J., Di Carlo, P., Lee, J. D., and Carpenter, L. J.: Interferences in photolytic NO$_2$ measurements: explanation for an apparent missing oxidant?, Atmos. Chem. Phys., 16, 4707–4724, https://doi.org/10.5194/acp-16-4707-2016, 2016.

Richter, A. and Burrows, J. P.: Tropospheric NO$_2$ from GOME measurements, in: Remote Sensing of Trace Constituents in the Lower Stratosphere, Troposphere and the Earth's Surface: Global Observations, Air Pollution and the Atmospheric Correction, edited by: Burrows, J. P. and Takeucki, N., Advances in Space Research, 11, Pergamon-Elsevier Science Ltd, Oxford, 1673–1683, 2002.

Richter, A., Burrows, J. P., Nuss, H., Granier, C., and Niemeier, U.: Increase in tropospheric nitrogen dioxide over China observed from space, Nature, 437, 129–132, https://doi.org/10.1038/nature04092, 2005.

Russell, A. R., Valin, L. C., and Cohen, R. C.: Trends in OMI NO$_2$ observations over the United States: effects of emission control technology and the economic recession, Atmos. Chem. Phys., 12, 12197–12209, https://doi.org/10.5194/acp-12-12197-2012, 2012.

Ryerson, T. B., Williams, E. J., and Fehsenfeld, F. C.: An efficient photolysis system for fast-response NO$_2$ measurements, J. Geophys. Res.-Atmos., 105, 26447–26461, https://doi.org/10.1029/2000jd900389, 2000.

Salmon, O. E., Shepson, P. B., Ren, X., He, H., Hall, D. L., Dickerson, R. R., Stirm, B. H., Brown, S. S., Fibiger, D. L., McDuffie, E. E., Campos, T. L., Gurney, K. R., and Thornton, J. A.: Top-Down Estimates of NO$_x$ and CO Emissions From Washington, DC-Baltimore During the WINTER Campaign, J. Geophys. Res.-Atmos., 123, 7705–7724, https://doi.org/10.1029/2018jd028539, 2018.

Silvern, R. F., Jacob, D. J., Travis, K. R., Sherwen, T., Evans, M. J., Cohen, R. C., Laughner, J. L., Hall, S. R., Ullmann, K., Crounse, J. D., Wennberg, P. O., Peischl, J., and Pollack, I. B.: Observed NO/NO$_2$ Ratios in the Upper Troposphere Imply Errors in NO-NO$_2$-O$_3$ Cycling Kinetics or an Unaccounted NO$_x$ Reservoir, Geophys. Res. Lett., 45, 4466–4474, https://doi.org/10.1029/2018gl077728, 2018.

Simon, H., Reff, A., Wells, B., Xing, J., and Frank, N.: Ozone Trends Across the United States over a Period of Decreasing NO$_x$ and VOC Emissions, Environ. Sci. Technol., 49, 186–195, https://doi.org/10.1021/es504514z, 2015.

Smith, J. B., Wilmouth, D. M., Bedka, K. M., Bowman, K. P., Homeyer, C. R., Dykema, J. A., Sargent, M. R., Clapp, C. E., Leroy, S. S., Sayres, D. S., Dean-Day, J. M., Bui, T. P., and Anderson, J. G.: A case study of convectively sourced water vapor observed in the overworld stratosphere over the United States, J. Geophys. Res.-Atmos., 122, 9529–9554, https://doi.org/10.1002/2017jd026831, 2017.

Souri, A. H., Choi, Y. S., Jeon, W. B., Li, X. S., Pan, S., Diao, L. J., and Westenbarger, D. A.: Constraining NO$_x$ emissions using satellite NO$_2$ measurements during 2013 DISCOVER-AQ Texas campaign, Atmos. Environ., 131, 371–381, https://doi.org/10.1016/j.atmosenv.2016.02.020, 2016.

Steinbacher, M., Zellweger, C., Schwarzenbach, B., Bugmann, S., Buchmann, B., Ordonez, C., Prevot, A. S. H., and Hueglin, C.: Nitrogen oxide measurements at rural sites in Switzerland: Bias of conventional measurement techniques, J. Geophys. Res.-Atmos., 112, D11307, https://doi.org/10.1029/2006jd007971, 2007.

Streets, D. G., Canty, T., Carmichael, G. R., de Foy, B., Dickerson, R. R., Duncan, B. N., Edwards, D. P., Haynes, J. A., Henze, D. K., Houyoux, M. R., Jacobi, D. J., Krotkov, N. A., Lamsal, L. N., Liu, Y., Lu, Z. F., Martini, R. V., Pfister, G. G., Pinder, R. W., Salawitch, R. J., and Wechti, K. J.: Emissions estimation from satellite retrievals: A review of current capability, Atmos. Environ., 77, 1011–1042, https://doi.org/10.1016/j.atmosenv.2013.05.051, 2013.

Strode, S. A., Rodriguez, J. M., Logan, J. A., Cooper, O. R., Witte, J. C., Lamsal, L. N., Damon, M., Van Aartsen, B., Steenrod, S. D., and Strahan, S. E.: Trends and variability in surface ozone over the United States, J. Geophys. Res.-Atmos., 120, 9020–9042, https://doi.org/10.1002/2014jd022784, 2015.

Thornton, J. A., Wooldridge, P. J., and Cohen, R. C.: Atmospheric NO$_2$: In situ laser-induced fluorescence detection at parts per trillion mixing ratios, Anal. Chem., 72, 528–539, https://doi.org/10.1021/ac9908905, 2000.

Tong, D. Q., Lamsal, L., Pan, L., Ding, C., Kim, H., Lee, P., Chai, T. F., Pickering, K. E., and Stajner, I.: Long-term NO$_x$ trends over large cities in the United States during the great recession: Comparison of satellite retrievals, ground observations, and emission inventories, Atmos. Environ., 107, 70–84, https://doi.org/10.1016/j.atmosenv.2015.01.035, 2015.

Travis, K. R., Jacob, D. J., Fisher, J. A., Kim, P. S., Marais, E. A., Zhu, L., Yu, K., Miller, C. C., Yantosca, R. M., Sulprizio, M. P., Thompson, A. M., Wennberg, P. O., Crounse, J. D., St. Clair, J. M., Cohen, R. C., Laughner, J. L., Dibb, J. E., Hall, S. R., Ullmann, K., Wolfe, G. M., Pollack, I. B., Peischl, J., Neuman, J. A., and Zhou, X.: Why do models overestimate surface ozone in the Southeast United States?, Atmos. Chem. Phys., 16, 13561–13577, https://doi.org/10.5194/acp-16-13561-2016, 2016.

Vinken, G. C. M., Boersma, K. F., Maasakkers, J. D., Adon, M., and Martin, R. V.: Worldwide biogenic soil NO$_x$ emissions inferred from OMI NO2 observations, Atmos. Chem. Phys., 14, 10363-10381, https://doi.org/10.5194/acp-14-10363-2014, 2014.

Wooldridge, P. J., Perring, A. E., Bertram, T. H., Flocke, F. M., Roberts, J. M., Singh, H. B., Huey, L. G., Thornton, J. A., Wolfe, G. M., Murphy, J. G., Fry, J. L., Rollins, A. W., LaFranchi, B. W., and Cohen, R. C.: Total Peroxy Nitrates ($\sum$PNs) in the atmosphere: the Thermal Dissociation-Laser Induced Fluorescence (TD-LIF) technique and comparisons to speciated PAN measurements, Atmos. Meas. Tech., 3, 593–607, https://doi.org/10.5194/amt-3-593-2010, 2010.

Xing, J., Mathur, R., Pleim, J., Hogrefe, C., Gan, C.-M., Wong, D. C., Wei, C., Gilliam, R., and Pouliot, G.: Observations and modeling of air quality trends over 1990–2010 across the Northern Hemisphere: China, the United States and Europe, Atmos. Chem. Phys., 15, 2723–2747, https://doi.org/10.5194/acp-15-2723-2015, 2015.

Zhang, L., Jacob, D. J., Knipping, E. M., Kumar, N., Munger, J. W., Carouge, C. C., van Donkelaar, A., Wang, Y. X., and Chen, D.: Nitrogen deposition to the United States: distribution, sources, and processes, Atmos. Chem. Phys., 12, 4539–4554, https://doi.org/10.5194/acp-12-4539-2012, 2012.

Zhang, R., Wang, Y., Smeltzer, C., Qu, H., Koshak, W., and Boersma, K. F.: Comparing OMI-based and EPA AQS in situ NO$_2$ trends: towards understanding surface NO$_x$ emission changes, Atmos. Meas. Tech., 11, 3955–3967, https://doi.org/10.5194/amt-11-3955-2018, 2018.